The Nocturnal Heat Island Formation and Rural Lapse Rates Based on Steep Slope Soundings in Nagano Basin, Japan

Shinshu University Journal of Educational Research and Practice, No.4, pp.99-112, 2011

<Academic paper>

The Nocturnal Heat Island Formation and Rural Lapse Rates Based on Steep Slope Soundings in Nagano Basin, Japan

SAKAKIBARA Yasushi Faculty of Education, Shinshu University
SATO Keiji Koshokunishi Junior High School, Chikuma, Nagano

Keywords: heat island, local climate, lapse rate, Nagano basin

1. Introduction

The air in the urban canopy is usually warmer than that in the surrounding country side. It is well known as an urban heat island effect (Oke, 1987). The heat of summer has interested from the unpleasantness in urban life and the study about the measure against urban heat island has recently been done. This heat island arose from the concentration of population to an place. Cities or town are built with the gathering of people.

The increase of anthropogenic heat and the material which has high competence in heat storage, the growth of water-proofing material, the change of urban geometry which brings large roughness and small sky view factor can be seen in urban areas. The existence of the material which increases thermal admittance, acts as a discouragement factor in heat island formation. But the existence of water proofing material decreases evapotranspiration and acts as an encouragement factor in heat island formation.

On the other hand heat storage heat stored in the day time and anthropogenic heat releases at night. They heat urban air. Since the wall is warmer than the sky, the existence of the building reduces the loss of the net long wave radiation on the opposite wall and street floor and their surface temperature become cool slowly. Thus urban air temperature is not easy to cool. Sakakibara and Sato (2008) showed that the temperature cooling amount from the sunset became smaller as the sky view factor of the city become smaller. In other words this effect was small and was not the main cause of heat island formation in the large sky view factor cities.

Generally speaking, the air is always moving. There is large difference in the sky view factor between the main street and the near back street. The air temperature is the averaged value in some extent of space, but the sky view factor is the index in a particular spot. Thus we must use the representative sky view factor in order to verify the effect of sky view factor on the heat island intensity (*HII*) and air temperature. There was no report about representative sky view factor in actual cities.

Anyway *HII* should become larger in a small wind speed, if heat island results from the heating from urban surface. But Sakakibara and Mieda (2002) reported that the wind speed in which the maximum *HII* occurred was about 1 or 2 m/s. Why such a fact can be seen? When wind speed becomes large the mechanism to promote the heat island formation should work until

a wind speed such as 1 or 2 m/s. For example, the mixing of the atmosphere happens in the rough urban surface when the wind blows. In the favor the air temperature at the screen level may go up, since the air at the screen level cooled by the radiation cooling mixed with warmer air at some higher level.

Tamiya and Ohyama (1981) discussed the mechanism of heat island formation from causes by the mechanical mixing of urban atmosphere and heating based on the observation of heat island in a small settlement. The result could not deny the mixing as the mechanism of occurrence of heat island. But there were no data of so weak wind as not to mix the air in urban area in their study. They told that such data would bring to the assessment of both courses, since the mixing did not cause the heat island in a calm condition and that the more the heating raised it up the weaker the wind in a calm condition.

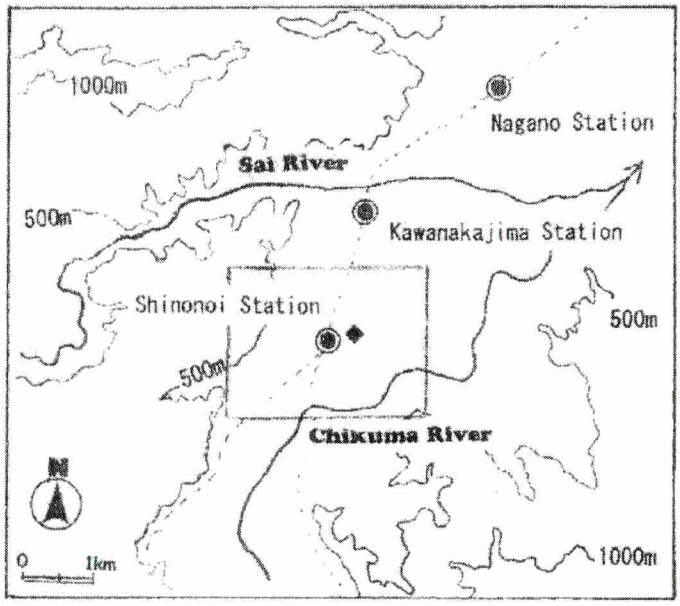

a

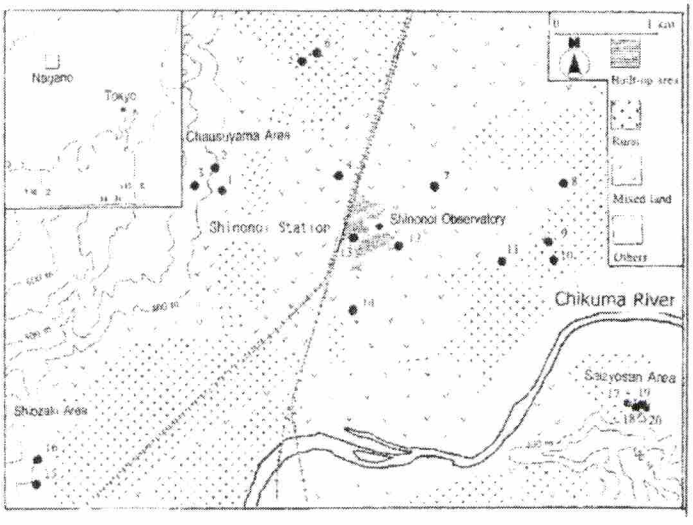

b

Figure 1 Base map of research area.

Sakakibara (2001) suggested that the mechanical mixing of urban atmosphere contributed to nocturnal heat island more than the heating urban surface in the small and middle cities, with comparison of the correlation coefficient between *HII* and Rural Lapse Rate (*RLR*), and between *HII* and the square of wind speed/*RLR*, the *HII* with *RLR* and wind speed and the *RLR* with wind speed. But there was no comment about the effect of heating from urban surface on

the heat island formation.

This study presented the discussion about the causes of nocturnal heat island in the settlement based on a case study attendant on observations on a calm condition.

2. Method

2.1 Research area

Observations were taken near Chausuyama (Fig. 1b, point 1-3, the ground surface inclination of 9 degree, E), Shiozaki (points 15 and 16, the inclination of 16 degree, E), and Saizyosan (points 17-20, the inclination of 19 degree, N) and Shinonoi (points 4-14) in the southern part of Nagano City, located within the Nagano Basin. The observation points in the farmer three areas were located on steeply sloped roads. No trees were near observation points on the road, allowing the air around the point to freely exchange with boundary layer air.

Measurements in Shinonoi were used to diagnose the strength of the heat island; observations in other areas measured the nocturnal surface inversion. The road was paved with asphalt and traffic density was light in this area. There were 1240 cars from 19:00 to 7:00 near point 1 in Fig. 1b (Nagano Prefectural Office, 2006). The urban district in Shinonoi area includes many two- to three-story buildings in both commercial and residential areas. According to Auer (1978)'s classification of land use type, the farmer was correspondent to the C1 type of "commercial" and the latter was the R2 type of "small residential".

The area's population was 17,280 (Dec. 1, 2004). Two observation points (points 5 and 6) were selected west of the urban area, in rural areas where orchards were predominant. Other rural points (9 and 10) were east of the urban area. These points were in rice paddy fields that were flooded at the end of May and drained at the end of September, when the rice was matured. Rice was harvested in October, leaving the paddy fields bare.

2.2 Observation method

Air temperatures were measured by a thermistor (Hioki EE Corp., Ueda, Japan, 9021-01) as the car moved sequentially past observation points. The thermistor was accurate to within ±0.2 °C. Measurements were taken as the car moved at about 10 m/s. The time constant was within 10 s at this wind speed. The ventilation was needed since the heat was accumulated in the radiation shield. We didn't use an electric fan but a wind caused by moving the automobile.

The sensor was connected to a handheld computer (Seiko-Epson, Suwa, Japan, HC-40). After the measurements, data were transferred via an RS232C cable to a desktop computer (NEC Corp., Tokyo, Japan, PC9821Ap). The sensor was located within a radiation shield constructed of a polyvinyl chloride (PVC) tube (107 mm diameter, 3 mm thick, 360 mm long). The radiation shield was covered with an aluminum sheet to suppress heating by radiation, and was connected to a second PVC tube (80 mm diameter, 3 mm thick, 3000 mm long) that was fastened to a rooftop carrier on the automobile. The radiation shield tube was 150 cm above the ground, about 50 cm over the edge of the automobile fender, making it unlikely that engine heat would influence the measurements (Sahashi, 1983). When the automobile arrived at the observation

points, the switch connected to the computer was pushed. Then twice measurements were done in 2 seconds interval.

2.3 Meteorological conditions on observation days

Ninety-five observations were recorded around 22:00 Local Time (LT) on clear and cloudy nights from 5 January 2004 to 12 December 2004 (Table 1). Because snow was not removed from roads in Saizyosan in winter, winter observations were not conducted in Saizyosan.

Meteorological data collected at the Shinonoi observatory at the Health Center of Nagano City are representative of the wind direction and speed in the research area (Fig. 1a, mark ◆)

Table 1 Meteorological data on observation days.

No	Date	Time	Cloud Amount	Wind Time		m/s
1	2004/1/5	2149-2253	3	22:00	C	0.1
2	2004/1/7	2137-2221	9	22:00	WSW	3.2
3	2004/1/12	2144-2226	9	22:00	W	1.9
4	2004/1/20	2147-2228	1	22:00	WSW	1.5
5	2004/1/26	2133-2219	4	22:00	WSW	0.7
6	2004/1/28	2135-2221	4	22:00	C	0.4
7	2004/1/31	2214-2257	1	23:00	ESE	1.1
8	2004/2/10	2159-2244	0	22:00	SW	0.6
9	2004/2/16	2135-2222	0	22:00	W	0.7
10	2004/2/18	2232-2324	0	23:00	WSW	1.5
11	2004/2/24	2155-2246	1	22:00	SSE	1.1
12	2004/2/25	2037-2124	3	21:00	WSW	1.6
13	2004/3/7	2155-2240	9	22:00	NW	0.7
14	2004/3/8	2200-2248	0	22:00	NW	1.1
15	2004/3/10	2125-2230	7	22:00	WSW	1.0
16	2004/3/13	2116-2221	0	22:00	N	1.4
17	2004/3/14	2135-2234	0	22:00	WSW	0.8
18	2004/3/15	2128-2229	9	22:00	W	0.6
19	2004/3/17	2130-2235	0	22:00	SSE	1.2
20	2004/3/31	2124-2225	0	22:00	ESE	0.5
21	2004/4/1	2124-2230	10	22:00	SW	1.2
22	2004/4/10	2135-2240	2	22:00	SW	0.8
23	2004/4/12	2141-2246	8	22:00	ENE	3.7
24	2004/4/15	2149-2255	0	22:00	SW	1.0
25	2004/4/17	2122-2230	0	22:00	C	0.3
26	2004/4/22	2119-2217	0	22:00	N	1.5
27	2004/4/25	2128-2231	2	22:00	NNE	2.1
28	2004/4/26	2119-2218	10	22:00	WSW	4.4
29	2004/4/29	2128-2231	0	22:00	SW	0.8
30	2004/5/6	2121-2225	0	22:00	WSW	3.9
31	2004/5/8	2134-2236	10	22:00	WSW	5.6
32	2004/5/12	2129-2232	8	22:00	SW	6.7
33	2004/5/18	2136-2239	8	22:00	W	1.2
34	2004/5/25	2136-2238	0	22:00	S	0.5
35	2004/5/26	2127-2233	9	22:00	NW	0.6
36	2004/6/2	2130-2234	9	22:00	N	1.3
37	2004/6/3	2124-2235	0	22:00	SW	2.8
38	2004/6/4	2132-2242	0	22:00	SW	1.6
39	2004/6/9	2134-2242	10	22:00	NE	1.5
40	2004/6/10	2129-2234	9	22:00	NE	1.6
41	2004/6/27	2136-2311	9	22:00	WSW	1.6
42	2004/6/28	2132-2242	9	22:00	NE	2.1
43	2004/6/29	2134-2239	10	22:00	E	0.5
44	2004/7/2	2142-2307	5	22:00	E	3.2
45	2004/7/14	2122-2234	0	22:00	E	2.6
46	2004/7/19	2123-2237	1	22:00	ENE	1.4
47	2004/7/20	2125-2228	0	22:00	NE	0.8
48	2004/7/22	2121-2228	8	22:00	NE	1.3
49	2004/7/23	2128-2232	8	22:00	NW	0.7
50	2004/7/26	2130-2235	1	22:00	SW	1.1
51	2004/7/27	2124-2234	0	22:00	C	0.2
52	2004/8/10	2121-2227	7	22:00	ENE	0.8
53	2004/8/11	2122-2226	1	22:00	C	0.2
54	2004/8/13	2126-2228	0	22:00	C	0.4
55	2004/8/19	2128-2230	5	22:00	SSW	6.5
56	2004/8/20	2121-2228	0	22:00	N	1.1
57	2004/8/25	2121-2227	5	22:00	WNW	0.9
58	2004/8/27	2120-2223	10	22:00	SSW	3.7
59	2004/8/28	2121-2227	9	22:00	SSW	5.2
60	2004/9/3	2133-2234	9	22:00	NNE	1.3
61	2004/9/6	2129-2231	5	22:00	ENE	0.8
62	2004/9/13	2121-2223	0	22:00	WSW	1.3
63	2004/9/15	2115-2219	0	22:00	SW	5.1
64	2004/9/19	2122-2222	1	22:00	WNW	0.5
65	2004/9/25	2116-2219	9	22:00	N	0.7
66	2004/9/26	2124-2225	9	22:00	ESE	1.4
67	2004/10/1	2122-2223	0	22:00	SW	3.0
68	2004/10/6	2125-2234	1	22:00	WSW	0.6
69	2004/10/7	2138-2240	2	22:00	SW	3.5
70	2004/10/10	2121-2223	1	22:00	SW	5.9
71	2004/10/13	2123-2222	9	22:00	NE	1.7
72	2004/10/15	2129-2227	0	22:00	WNW	0.7
73	2004/10/16	2119-2218	1	22:00	NNW	0.6
74	2004/10/18	2127-2229	9	22:00	SW	5.0
75	2004/10/24	2126-2230	1	22:00	SW	2.2
76	2004/10/25	2122-2224	5	22:00	C	0.4
77	2004/10/28	2123-2227	0	22:00	SSE	1.4
78	2004/11/2	2128-2229	9	22:00	SW	0.9
79	2004/11/4	2124-2222	0	22:00	C	0.4
80	2004/11/5	2121-2223	2	22:00	C	0.1
81	2004/11/6	2126-2228	9	22:00	SSW	1.6
82	2004/11/8	2121-2220	0	22:00	WSW	2.4
83	2004/11/9	2118-2224	0	22:00	SSW	2.2
84	2004/11/17	2134-2236	0	22:00	SW	0.5
85	2004/11/23	2125-2230	0	22:00	SW	2.1
86	2004/11/25	2124-2228	4	22:00	SSE	0.7
87	2004/11/27	2127-2232	0	22:00	N	0.6
88	2004/11/30	2135-2242	0	22:00	NW	0.5
89	2004/12/1	2130-2235	1	22:00	N	1.0
90	2004/12/2	2129-2233	0	22:00	SW	1.3
91	2004/12/3	2123-2226	0	22:00	WSW	1.4
92	2004/12/8	2126-2234	0	22:00	C	0.2
93	2004/12/10	2132-2242	0	22:00	WSW	0.7
94	2004/12/11	2132-2243	9	22:00	N	0.9
95	2004/12/12	2128-2231	10	22:00	SSW	2.7

since the Shinonoi observatory was located at the center part of the research area. The anemometer sensor was mounted on a tower on the roof of a two-story building. The sensor was

20 m above the ground. Cloud cover was observed at point 3, where the sky view was unobstructed in all directions.

2.4 Heat island intensity

We selected the urban point and the rural point to calculate the *HII*, which was defined as Tu-Tr. Both of points were selected, based on the following criteria: the scenery around the points was typical of either urban or rural scenery in the field survey and the vegetation index of an urban point and a rural point was the minimum or the maximum in the research area. Thus, point 13 and point 6 were selected as an urban point and a rural point, respectively. The vegetation index was defined the proportion of vegetation area to the object area. In this study the object area was adopted the area of the 250 meters square centered at the observation point. Thus *HII* was defined as the temperature difference between point 13 and point 6.

2.5 Pseudo vertical sounding profiles

Observations on the steeply sloped roads were conducted in three areas using an automobile. The maximum round-trip time was less than 10 minutes, so it is likely that the temperatures that are measured at a point when the car is ascending are similar to those measured when the car is descending. In fact, if the temperature difference at a point between ascent and descent differed by more than 0.5 °C, the data were considered erroneous.

In Chausuyama, 59 out of 95 runs were selected. Twenty-six cases had no errors in three steep slope soundings. The average of the temperature measured on descent and on ascent was used in the analysis. The lapse rate was calculated as follows:

$$\theta_z = T(z) + \Gamma_d (z - z_{std}) , \tag{1}$$

where θ_z and $T(z)$ denote the potential temperature and air temperature at height z, Γ_d and z_{std} are the dry adiabatic lapse rate (0.00977 °C/m) and standard altitude, respectively. The potential temperature of a parcel is the value it would have if it were at the arbitrary pressure value of 1000 hPa and its altitude is regarded as the standard altitude. But the standard altitude was not used in the following calculation.

The potential temperature difference between altitude z_a and z_b is:

$$\Delta\theta = T_a - T_b + \Gamma_d (z_a - z_b), \tag{2}$$

where T_a and T_b are the temperatures at z_a and z_b. Thus, the lapse rate α is:

$$\Delta\theta / (z_a - z_b) = (T_a - T_b) / (z_a - z_b) + \Gamma_d . \tag{3}$$

Figure 2 shows the pseudo vertical temperature profiles that were based on steep slope

soundings at Chausuyama. The potential temperature difference was calculated from equation (3). The sample number is 59. Mean values are shown by the dotted line. A horizontal line denotes an error bar (standard deviation). The temperature at 360 m above sea level was the lower than that at 380 m, 400 m, and 420 m (significant in 1% level, $P < .01$). As height increased, the average of potential temperature differences increased and the lapse rate became small.

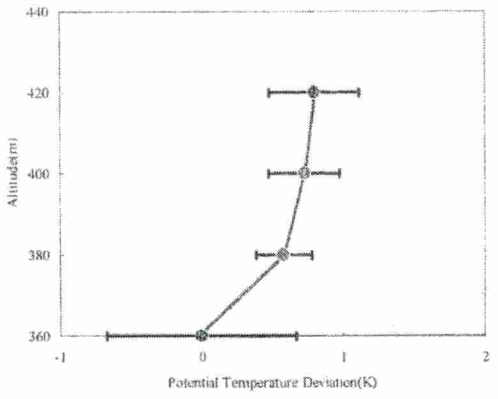

Figure 2 Pseudo vertical temperature profile observed by a car moving along a steep slope road in Chausuyama.

3. Mean temperature anomaly and the altitude of the moving observation route

The temperature distribution along the observation route was obtained by calculating the temperature anomaly for each point. Then, the 91 runs were split into two categories, clear days (cloud cover < 9; 68 runs) and cloudy days (cloud cover = 9 or 10; 25 runs), because there is the difference of radiation cooling in both of days. At each point, the average temperature anomaly and the standard deviation of the temperature anomaly were calculated (Fig. 3). The horizontal axis in Figure 3 denotes the distance from point 1 and the numbers represent the observation points. The average temperature anomaly is denoted by ■ for rural points, □ for urban points, and ▒ for mixed land use points. Vertical bars indicate the standard deviation of the temperature anomaly. The dotted line shows the altitude profile of the

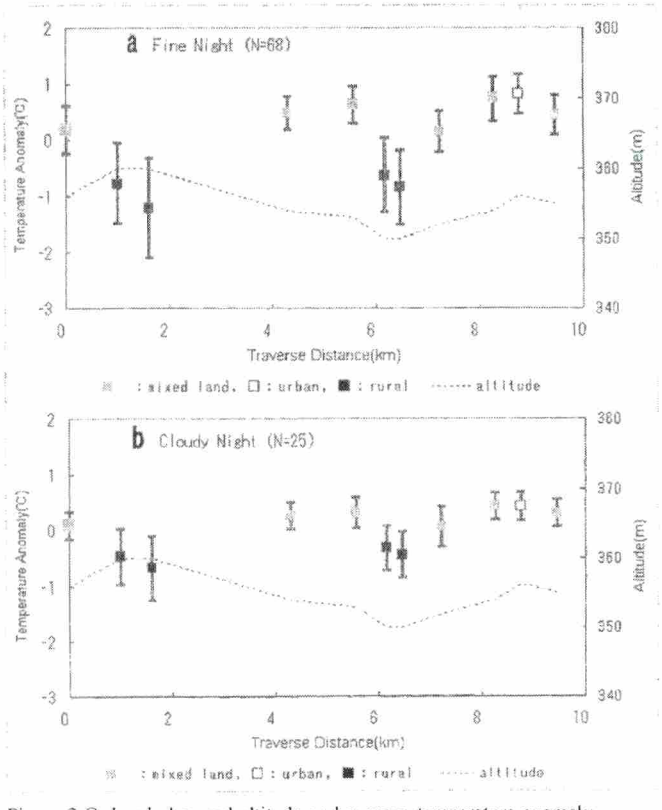

Figure 3 Ordered observed altitude and average temperature anomaly. N denotes the sample number.

observation route.

Because the maximum altitude difference between one site and another was, at most, 10 m, no correction was applied for the height difference. Urban areas were warmer than rural areas. Point 6 was the coldest of all of the points. Temperature difference patterns on clear nights were similar to the patterns on cloudy nights. The temperature difference between sites was larger on clear nights than it was on cloudy nights. Since there was small difference of downward long wave radiation between urban and rural on cloudy nights, urban geometry may not play on important role in nocturnal heat island formation on cloudy nights. This result agreed with the previous reports (*ex.* Oke (1987)).

4. Air temperature and lapse rate of potential temperature above a rural area

Air temperatures above a rural area were compared using 27 runs in which all of the temperature differences at points measured on ascent and on descent on steep slopes were smaller than 0.5 °C (Table 2). We average the round trip temperatures at each observation point. There were small differences in the 400 m temperature among the three slopes. The 380 m temperature of the Shiozaki slope was similar to that of the Chausuyama slope, but about 0.2 °C cooler than that of the Saizyosan slope. Temperatures at 370 m and 390 m were similar to those at 380 m on the Saizyosan slope. It may be due to the same direction. The Shiozaki slope and the Chausuyama slope are the same direction. On the other hand the Saizyosan slope is opposite direction to other slopes.

Table 2 Average temperature on three steep slopes.

Altitude(m)	Shiozaki	chausuyama	Saizyosan
400	13.2	13.2	13.2
390			13.0
380	13.3	13.3	13.0
370			13.0

Lapse rates at three rural areas were compared. The method used to determine the lapse rate is important because smaller lapse rates occur at higher altitudes, and higher buildings may have a greater affection on the urban atmosphere. The Japan Railway Shinonoi Station building, which height is 353 m above sea level, rises about 13 m above the ground, and was the highest in this research area. Most other buildings rose about 7 m above the ground. If the height at which a building can affect the urban atmosphere is about twice the height of the building, this influence ranges from 14 m to 26 m. The potential temperature gradient α based on temperatures at 360 m and 380 m above sea level was considered to be a lapse rate. Point 6, which height is 359 m above sea level, had the coldest average temperature of all of the points and was most frequently the coldest point. The lapse rate at point 6, which was selected as a rural point in a previous chapter, was calculated using the temperature there, and the temperatures on the steep slope at sounding points 2, 15, and 18, at 380 m above sea level (20 m above the ground).

Table 3 Lapse rate based on a car moving observation along three steep slope roads.

Cloud Cover	Lapse rate(°C/m) Shiozaki	chausuyama	Saizyosan
0 – 8	0.048	0.047	0.019
9, 10	0.005	0.008	−0.009

Data were used from 45 runs in which the temperature difference between all of the

measurements at a point on ascent and descent was less than 0.5 °C on three steep slopes. The 45 cases were split into two categories: clear nights (N = 30) and cloudy nights (N = 15). In all of the cases, the lapse rate on small cloud cover days was greater than that on large cloud cover days (Table 3). The lapse rate near Shiozaki was similar to the lapse rate near Chausuyama, but not similar to that near Saizyosan (significant in 5 % level).

This suggested that rural vertical temperature profiles might vary with the area even if they located in the same basin. Generally speaking there is mountain and valley breeze in the mountain slope area. Since the heat radiates from the slope, the slope and the air above it become cold. The cold air drainage occurs, and the basin area becomes cold, too. The evening heat storage of slopes from the solar radiation may vary with the slope direction. It may bring about the different temperature area horizontally in the same basin area. The *RLR* in Chausuyama slope observation was selected of three *RLR*s on discussion about the mechanism of heat island formation. The dispersion in the figure described later was smaller than that used by other *RLR*s. The result in this choice was similar to that used by other *RLR*s.

5. Rural lapse rate and mechanism of heat island formation

Figure 4 compares *HII* and *RLR* based on the Chausuyama pseudo vertical temperature profile. *RLR* was calculated using temperatures at point 6 and point 2. Data were from 68 runs in which the air temperature difference at point 2 for ascending and descending measurements was smaller than 0.5 °C. A larger *RLR* accompanies a greater *HII*. Tamiya and Ohyama (1981) described a nocturnal heat island model in which a temperature excess was produced by preventing the formation of the inversion layer in the urban area from developing. They hypothesized that nocturnal temperature increases near the urban surface arose from either (1) the heating from urban surface that forces

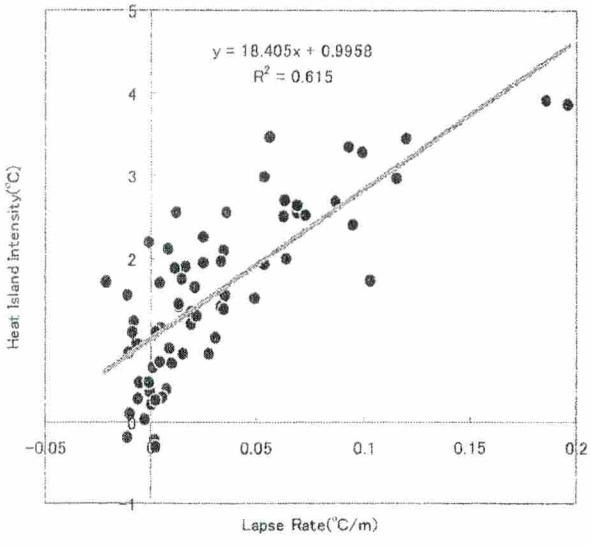

Figure 4 Heat island intensity vs. lapse rate as derived from Chausuyama pseudo vertical profiles.

the formation of a neutral (constant potential temperature) layer at height of 0 – h, or (2) the mechanical mixing, related to the large roughness of urban surfaces, that forces the formation of a neutral layer at height of 0 – $2h$ (Fig. 5). Observational results in this study were applied to their heat island model. The heating from urban surface originated from anthropogenic heat and increased sensible heat storage in urban area.

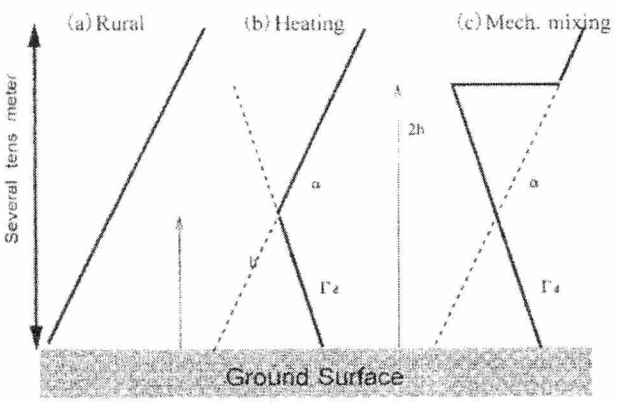

Figure 5 Schematic chart of surface inversion destruction.

5.1 Mechanism of the heat island formation by the heating from urban surface

We traced the heat island model of Summers (1965) in the case of the heating from the urban surface. Surface heat flux ΔQ, which is necessary for the warming of $\delta T(z)$ to the height h at the down stream distance X under the wind velocity u, is

$$\Delta Q = \frac{u}{X}\int_0^h \rho C_p \delta T(z)\,dz \quad , \tag{4}$$

$$\delta T(z) = T(h) + (h - z)\,\Gamma_d - T(z) \, , \tag{5}$$

Here, ρ and C_p denote the density of the dry air and specific heat at constant pressure, respectively.

On the assumption of linear temperature distribution ($\Delta T = (T(h) - T(z))/(h - z)$, constant) in the inversion layer, $\delta T(z)$ is simplified to

$$\delta T(z) = (h - z)(\Gamma_d + \Delta T) \quad , \tag{6}$$

then ΔQ, h and $\delta T(0)$, warming at surface *i.e. HII*, can be respectively, obtained from the following equation,

$$\Delta Q = \frac{u}{2X}\rho C_p(\Gamma_d + \Delta T)h^2 \quad , \tag{7}$$

$$h=\sqrt{\frac{2\Delta QX}{\rho C_p u(\Gamma_d+\Delta T)}}\quad , \tag{8}$$

and

$$\delta T(0)=\sqrt{\frac{2\Delta QX(\Gamma_d+\Delta T)}{\rho C_p u}}\quad . \tag{9}$$

Since $\delta T(0)$ was temperature difference between urban and rural on the ground, $\Delta T(z) = HII$. Substituting $\alpha=\Gamma_d+\Delta T$, HII is obtained from the following equation,

$$HII=\sqrt{\frac{2\Delta QX}{\rho C_p}}\sqrt{\frac{\alpha}{u}}\quad . \tag{10}$$

The relationship between HII and $(\alpha/u)^{1/2}$ based on 68 runs in which the temperature differences at point 2 measured on ascent and on descent was shown in Fig. 6. The open circles denote the case on the wind speed under 0.2 m/s. Considering the accuracy of the anemometer, these plots were not more reliable than others. A regression line was calculated by using data except open circles ($r^2=0.6239$). Since the gradient of this regression line corresponded to

$$\sqrt{\frac{2\Delta QX}{\rho C_p}}=6.7\quad . \tag{11}$$

The intercept of the y-axis results from the factor except the heating from urban surface. Substituting the size of settlement $X=1000$ m, $\rho=1.204$ kg m^{-1} (for 20 °C), $C_p=1010$ Jkg^{-1}°C^{-1} for eq. (11), $\Delta Q=27.4$ W/m^2. If we used the air density for 0 °C, $\Delta Q=29.5$ W/m^2. Judging from the report that the average heat flux of Tokyo metropolitan area was over 10 W/m^2 (Fujibe, 1998), it may be unreasonable to anticipate that there was such a large heat flux in a small settlement like Shinonoi area which population was 17,280.

5.2 Mechanism of the heat island formation by the mechanical mixing

HII is defined as:

$$HII = \alpha h, \tag{12}$$

where α and h are the RLR and the height of the crossing point of the constant potential temperature layer and the inversion layer, respectively. The lapse rate in the rural air is smaller than in the dry adiabatic Γ_d by an amount α. The gradient of regression in Figure 4 corresponds to h; h is 18.4 m.

We considered the height of the crossing point of the constant potential temperature layer

and the inversion layer, which corresponded the height of the urban mixing layer at night. The height is affected by the average of building height and meteorological conditions. Roth (2000) reported that buildings could affect the urban atmosphere at heights 2 to 2.5 times greater than the building height.

He did not discuss which of the heating from urban surface and the mechanical mixing was the main cause of heat island. But we notice only the energy of mixing derive from wind. It is not cleared up whether the height of urban atmosphere affected by a building varies with a wind speed. We supposed the height constant for simplicity.

When wind flows from rural areas, where surface inversion layers exist on calm, clear nights, to urban areas, urban buildings cause a change in wind direction, including the vertical wind direction. The urban atmosphere is thus stirred and acquires a constant potential temperature under $2h$. When wind entered the urban area, the wind speed decreases from u_1 (the rural wind speed) to u_2 (the urban wind speed). If the mixing occurs in the layer between $0 - 2h$, the change in kinetic energy per unit area is:

$$\int_0^{2h} \left(\frac{1}{2}\rho u_1^2 - \frac{1}{2}\rho u_2^2\right) dz = \bar{\rho}\left(\bar{u_1}^2 - \bar{u_2}^2\right) h \quad , \tag{13}$$

where ρ is the air density. The over bar denotes the average in the $0 - 2h$ layer. This result is based on similar assumptions in Summers (1965) for the vertical wind profile in urban and rural locations. A bold assumption might be set up for simplicity as follows; a simple linear increase of temperature with height exists in the country; the mean wind up to a height of $2h$ over the city is equal to the mean wind up to the same height in the country; because the air in the adiabatic layer is in a vertical circulation, there will be a uniform wind under a height of $2h$.

The vertical circulation in the adiabatic layer forces the constant potential temperature profile to a height of $0 - 2h$ (Fig. 5c, solid line). The heat in the layer from h to $2h$ descends to the layer from 0 to h. Work W based on the mixing is:

$$W = g\int_0^{2h} (\rho_\Gamma(z) - \rho(z)) z\, dz \quad , \tag{14}$$

where g, $\rho_\Gamma(z)$, and $\rho(z)$ are the gravitational acceleration, the density at height z in the layer with constant potential temperature, and the density at height z in the inversion layer, respectively. Equation (14) can be solved using a statics equation and the ideal gas equation, yielding the work W due to mixing:

$$W = \frac{2\bar{\rho} g \alpha h^3}{3\bar{T}} \quad . \tag{15}$$

Then we regard the energy loss of friction and the energy increase caused by the change of the vertical wind profile as of little value.

Setting the right hand term in (13) equal to the right hand term in (15) yields:

$$\bar{u}_2 = \sqrt{\bar{u}_1^2 - \frac{2g\alpha h^2}{3\bar{T}}} \quad . \tag{16}$$

When the urban wind speed u_2 approaches 0, rural wind u_1 approaches u_0 as:

$$u_0 = \sqrt{\frac{2g\alpha h^2}{3\bar{T}}} \quad . \tag{17}$$

This equation corresponded to the model of Tamiya and Ohyama (1981) and represented the minimum wind speed needed the formation of a neutral layer in urban. If the rural wind speed is under u_0, the urban wind speed u_2 become 0. So the mixing over urban area becomes very weak. If u_1 changes within the limits of 10 %, the result based with equation (13) and (15) shows that u_0 changes within those of 10 %.

In actually, even if rural wind speed is smaller than u_0, vertical profile of temperature in urban area may not instinctively the shape like Fig. 5(c) but an intermediate style between Fig. 5(a) and (c), because urban atmosphere mixed somewhat in such a case. The *HII* in the halfway mixture condition may be smaller than that in perfect. This suggests that *HII* becomes large until a wind speed when a wind speed increase.

A heat island will not be present when strong wind destroys the surface inversion layer in both rural and urban areas. The strength of such a wind is unknown, but if the energy involved in a 1 % wind speed decrease is enough to destroy both urban and rural surface inversions, the corresponding rural wind speed u_{99} is:

$$u_{99} = \sqrt{\frac{2g\alpha h^2}{3\bar{T}(1-0.99^2)}} \quad . \tag{18}$$

Since urban wind speed u_2 is supposed to be 99 % of rural wind speed u_1, u_1 and u_2 are regarded to have the same change tendency. When u_1 and u_2 increase (decrease) at the rate of 10 %, u_{99} increases (decreases) at the rate of 10 %.

Figure 6 shows the relationship between *RLR* and wind speed. Symbols of circle and dotted lines denote observation values and the graphs of u_0 and u_{99}. A temperature of 273 K (for night in late fall) and h of 18.4 m (from Fig. 4) are assumed. A value of g is constant. If *RLR* (= α) changes from 0 to 0.2, we can get the graphs of u_0 and u_{99} by using equation (17) and (18). The

larger the wind speed, the smaller the *RLR*. Then the surface inversion did not occur clearly. When the wind speed was small, all *RLR* was not large. The *HII* over 3 °C occurred when *RLR* was over 0.5 °C/m. The maximum *RLR* appeared at the wind speed of 2.2 m/s, and the second appeared at 2.1 m/s. The maximum and second *HII* appeared at the same time. Some wind might blow in the optimum weather condition that heat island appeared clearly. This was correspondent to Sakakibara and Mieda (2002).

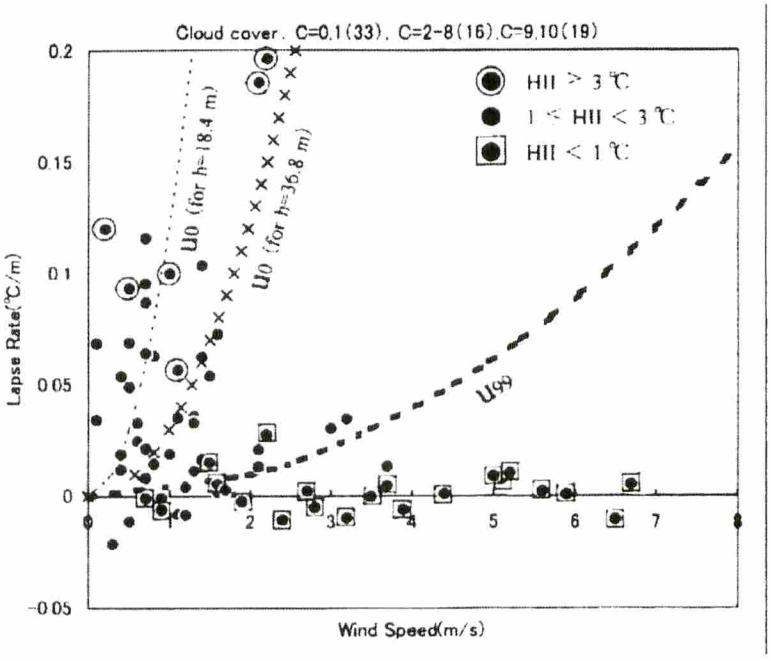

Figure 6 Relation between wind speed and lapse rate.

The limit of wind speed u_0 that heat island was caused by the effect except mixing was shown in Fig. 9. The u_0 depends on h as shown in eq. (9). The value of h was estimated from the gradient of Fig. 8. But h was not always the same actually. The value of u_0 calculated by using the double value in h was shown in Fig. 9. If h varied in a double value, *HII* over 3 °C was located in zone under u_0. This suggested that the cause that heat island appeared clearly was except the mixing. When paying to *RLR* over 0.5 °C/m in Fig. 8, h was smaller than 18.4 m. As the observation site of wind was located at urban area rather than rural. The wind speed used in this study may be underestimated as a rural one. Thus the result can deny the effect of mixing as the cause of heat island.

6. Conclusions

Temperature observations recorded by an automobile along three steep slopes in Nagano Basin, Japan, are used to describe the properties of nocturnal temperatures and rural lapse rates and the mechanisms of nocturnal heat island formation.

It was shown that heat island did not appear clearly when the rural lapse rate was small, regardless of the magnitude of wind speed and that the result can not deny the effect of the mixing on the heat island formation.

The wind speed used in this study, however, was not for a typical rural area but for an urban area. The rural wind speed may be underestimated, and anemometer measurements at a typical rural location are perhaps warranted. In addition, more extensive field observations, including temperature and vertical wind profiles, must occur in both urban and rural settings to verify the nocturnal heat island hypothesis.

Acknowledgements

The authors thank anonymous referees for useful comments for the manuscript in revising paper.

References

Auer, A.H.Jr., 1978: Correlation of land use and cover with meteorological anomalies, *J. Appl. Meteorol.*, **17**, 636-643.

Fujibe, F., 1998: Urbanization makes climate change. *Kagaku*, 68(3), 238-345, (in Japanese).

Nagano prefectural Office, 2006; Reports of Road Traffic Census 2005, Nagano Prefectural Office, 1-418, (in Japanese).

Oke, T.R. 1987: *Boundary layer climate*, 2nd Edition, Routledge, NewYork, 1-435.

Roth, M., 2000: Review of atmospheric turbulence over cities, *Quart J of Roy Meteor Soc* **126**, 941-990

Sahashi, K., 1983: Errors in the air temperature observation by traveling method with the automobiles - Effects of the automobiles, *Tenki*, **30**, 509-514, (in Japanese).

Sakakibara, Y., 2001: Comparison between the effect of heating from urban surface and that of mechanical mixing of urban atmosphere to heat island, *Tenki*, **48**, 305-311, (in Japanese with English abstract).

Sakakibara, Y. and Mieda, A., 2002: Cause of nocturnal heat island and the difference between *HII* on fine and cloudy days, *Tenki*, **49**, 533-540, (in Japanese with English abstract).

Sakakibara, Y. and Sato, T., 2008: Relationship between urban - rural temperature differences after sunset and urban geometry, *Geographical Reports of Tokyo Metropolitan University*, **43**, 57-68.

Summers, P.W., 1965: An urban heat island model; its role in air pollution problems, with applications to Montreal. Paper presented to the "First Canadian conference on micrometeorology" in Toronto, 12-14 April, 32 pp.

Tamiya, H. and H. Ohyama, 1981: Nocturnal heat island of small town, its manifestation and mechanism, *Geographical Review of Japan*, **54**-1, 1-21, (in Japanese with English abstract).

(2010年10月19日　受付)
(2011年 2 月15日　受理)

Reprinted from ***Shinshu University Journal of Educational Research and Practice.*** No. **4,** p99~112, 2011.